

Filament Stretching Rheometer: Inertia Compensation Revisited

Peter Szabo¹ Gareth H. McKinley²

¹ Danish Polymer Centre, Department of Chemical Engineering, Technical University of Denmark, Building 423, DK-2800 Kongens Lyngby, Denmark; e-mail: ps@kt.dtu.dk

² Department of Mechanical Engineering, Massachusetts Institute of Technology, Cambridge, Massachusetts 02139, USA; e-mail: gareth@mit.edu

23rd May, revised 29th Aug, 2002

Abstract

The necessary inertia compensation used in the force balance for the filament stretching rheometer is derived for an arbitrary frame of reference. This enables the force balance to be used to correctly extract the extensional viscosity from measurements of the tensile force at either end of the elongating fluid column in any of the different experimental configurations that have been introduced to date. The present analysis eliminates a restriction inherent in the work of Szabo, *Rheol. Acta*, **36**: 277-284 (1997).

Key words: Filament stretching rheometer, force balance, inertia compensation, extensional viscosity.

Introduction

Over the past decade, filament stretching rheometers have been used increasingly as a means for accurately measuring the transient uniaxial extensional viscosity of viscoelastic fluids (McKinley and Sridhar, 2002). A fluid filament is formed between two rigid end-plates and elongated by a rapid separation of the plates. A force transducer attached to one or other of the plates measures the tensile force generated by the elongation and a laser micrometer measures the evolution in the radius of the fluid column at the axial midplane. A number of different experimental configurations have been introduced and it is helpful to derive a general force balance which can be adapted to each different configuration. This was first done rigorously by Szabo (1997) and the resulting force balance was successfully used in an international study to compare experimental measurements of the transient extensional viscosity of a common test fluid in three differently-configured filament stretching devices (see Anna *et al.* 2001). The test fluids used in this work, and in most other experimental filament stretching studies to date, have been quite viscous (typically with viscosities greater than $\eta_0 > 1$ Pa.s), in order to minimize the influence of gravitational sagging in the filament. As a consequence, inertial effects have also typically been very small for the range of stretch rates that can be accessed experimentally. However as experiments begin to focus on dilute polymer solutions in lower viscosity solvents, an accurate treatment of inertial effects is becoming increasingly important. In this note we generalize the previous work by Szabo to develop a general force balance for filament

stretching devices that is correct even in arbitrary non-inertial reference frames such as those configurations commonly used in experiments.

An arbitrary frame of reference

In Figure 1 we define the basic geometrical variables in the filament stretching rheometer. The derivation on page 278 in Szabo (1997) assumes implicitly that the filament geometry is located in an inertial frame of reference where the center plane is stationary at $z = 0$. To generalise the analysis we assume here that the upper half part of the filament is located between $z_0(t)$ and $z_0(t) + L(t)/2$ instead of the interval 0 to $L/2$. The local origin $z_0(t)$ located at the middle of the filament may be accelerating (typically axially) with respect to an external and stationary (inertial) frame of reference $\{r, z\}$. Three cases are encountered commonly in filament stretching experiments:

- (i). Both plates accelerate symmetrically in opposite directions with user-imposed profiles $\pm \dot{L}(t)/2$ such that the axial midplane remains stationary at $z = 0$ and the radius decreases exponentially in time.
- (ii). The bottom plate remains stationary and the top plate accelerates upwards at $+\ddot{L}(t)$. The midplane thus also accelerates upwards at $\ddot{z}_0 = +\ddot{L}(t)/2$.
- (iii). The top plate remains stationary and the lower plate accelerates downwards at $-\ddot{L}(t)$.

The principal reason for these different configurations is the fragility of the sensitive force transducers used to make measurements of the (small) tensile forces in the slender fluid columns (typically $R \sim O(1 \text{ mm})$). The transducers are very susceptible to imposed (exponentially-increasing) accelerations, and they are thus typically located on the stationary endplate in each configuration. It is therefore also important in developing the force balance to provide a mechanism for interconverting between the tensile forces exerted on each of the two endplates.

These considerations lead to a modification of the equation (6) in Szabo (1997) so that the general force balance in an external and inertial frame of reference for the top half of the fluid column now becomes the following,

$$\begin{aligned} & \langle \tau_{zz} - \tau_{rr} \rangle_s + \frac{1}{2} \langle \tau_{rr} - \tau_{\theta\theta} \rangle_s + \frac{1}{2} \langle r \tau_{zr} \rangle'_s \\ & = \frac{\rho g V_0}{2\pi R_s^2} + \frac{F_{p,top}}{\pi R_s^2} + \frac{\sigma}{R_s} (1 + R_s R_s'') + \rho \left(\frac{1}{R_s^2} \frac{d^2}{dt^2} \int_{z_0}^{z_0+L/2} z R^2 dz - \frac{1}{4} R_s \ddot{R}_s \right) \end{aligned} \quad (1)$$

where $F_{p,top}$ is the force measured on the top plate defined by:

$$F_{p,top} = \int_{S_p} \pi_{zz} dS - \pi R_p^2 p_a - \frac{2\pi\sigma R_p}{\sqrt{1 + (R_p')^2}} \quad (2)$$

In equation (1) dots and primes represent time and spatial (z) derivatives respectively. A variable in brackets, $\langle \rangle_s$ denotes an area average across the midfilament plane.

The modification, compared to the force balance in Szabo (1997), appears only in the inertia integral on the right of equation (1) where $z_0(t)$, the present location of the filament center plane, now enters the integration limits.

To simplify the analysis, we may want to compute the inertia integral in a frame of reference moving with the center plane. That is, we define and introduce a new local axial filament co-ordinate $x = z - z_0(t)$. The inertia integral then becomes,

$$\frac{d^2}{dt^2} \int_{z_0}^{z_0+L/2} z R^2 dz = \frac{d^2}{dt^2} \int_0^{L/2} x R^2 dx + \frac{\ddot{z}_0 V_0}{2\pi}. \quad (3)$$

The additional term is somewhat analogous to the ‘added mass’ term that appears in the Navier-Stokes equations when studying problems involving transient accelerations. Combining the equations (3) and (1) we obtain a general force balance which has the following form:

$$\begin{aligned} & \langle \tau_{zz} - \tau_{rr} \rangle_s + \frac{1}{2} \langle \tau_{rr} - \tau_{\theta\theta} \rangle_s + \frac{1}{2} \langle r \tau_{zr} \rangle'_s \\ &= \frac{\rho(g + \ddot{z}_0)V_0}{2\pi R_s^2} + \frac{F_{p,top}}{\pi R_s^2} + \frac{\sigma}{R_s} (1 + R_s R_s'') + \rho \left(\frac{1}{R_s^2} \frac{d^2}{dt^2} \int_0^{L/2} x R^2 dx - \frac{1}{4} R_s \ddot{R}_s \right) \end{aligned} \quad (4)$$

From this equation we note that if the center plane is fixed (case (i) in the list above) then there is no correction to the original force balance. If, however, the chosen configuration involves acceleration of the midplane then there will be a modification. If the bottom plate is fixed and only the top plate accelerates (case (ii) above) then a correction term with $\ddot{z}_0 = +\ddot{L}/2$ appears in equation (4). Conversely, if the upper plate is held stationary then a correction term with $\ddot{z}_0 = -\ddot{L}/2$ enters the expression. As the equation (4) is generally valid for any choice of $z_0(t)$, future stretching schemes, other than cases (i)-(iii) above, may in a simple way be directly accounted for.

The result in equation (4) may alternatively be developed for the force exerted on the bottom plate. The force, $F_{p,bottom}$ is defined by

$$F_{p,bottom} = \int_{S_{p,bottom}} \pi_{zz} dS - \pi R_p^2 p_a - \frac{2\pi\sigma R_p}{\sqrt{1 + (R_p')^2}}. \quad (5)$$

By extending the force balance to the entire fluid column rather than just the upper half, the analysis leads to the following general relationship between the two force measurements,

$$F_{p,top} = F_{p,bottom} - \rho(g + \ddot{z}_0)V_0. \quad (6)$$

From this relation we note that the two force readings become identical if the center plane has a *downwards* acceleration equal in magnitude to the gravitational acceleration g . This is the case of ‘free fall’. However, it is important to note that in general for the extensional profiles imposed in experiments, the length $L(t)$ increases approximately exponentially or faster, and thus so does the acceleration at the midplane (McKinley and Sridhar (2002)).

To illustrate the importance of this additional inertial correction term, we consider the simplest case of ideal uniaxial elongation. In this case, the length increases as $L(t) = L_0 \exp(\dot{\epsilon}_0 t)$ and the radius decreases as $R(t) = R_0 \exp(-0.5\dot{\epsilon}_0 t)$ such that the volume of the fluid column is a constant $V_0 = \pi R_0^2 L_0$. If the filament is initially under quiescent conditions so that all stresses are identically zero, then the only stress components that develop during the subsequent elongation are those in the first term on the left-hand side of eq. (4). Denoting the transient extensional viscosity by $\eta_E^+ \equiv -\langle \tau_{zz} - \tau_{rr} \rangle_s / \dot{\epsilon}_0$ and substituting into eq. (4) leads to the following expression

$$\eta_E^+ = \frac{-F_{p,top}}{\pi R_0^2 \dot{\epsilon}_0} e^{\dot{\epsilon}_0 t} - \frac{\rho(g + \ddot{z}_0)V_0}{2\pi R_0^2 \dot{\epsilon}_0} e^{\dot{\epsilon}_0 t} - \frac{\sigma}{R_0 \dot{\epsilon}_0} e^{0.5\dot{\epsilon}_0 t} - \frac{\rho \dot{\epsilon}_0 L_0^2}{8} e^{2\dot{\epsilon}_0 t} + \frac{\rho \dot{\epsilon}_0 R_0^2}{16} e^{-\dot{\epsilon}_0 t} \quad (7)$$

The force on the lower plate can be found if desired using eq. (6). The negative sign on the force term is correct because the force $F_{p,top}$ is defined as shown in Figure 1. In general, for experiments, the net tensile force from the elongating fluid column will act downwards on the top plate (*i.e.* it will be negative). It is clear from equation (7) that the axial inertia term becomes increasingly important at long times or large Hencky strains. However the term arising from the acceleration of the reference frame is also of the same order as this term. In general terms we can let $\ddot{z}_0 = a\ddot{L} = a\dot{\epsilon}_0^2 L_0 e^{\dot{\epsilon}_0 t}$. Equation (7) then becomes

$$\eta_E^{\pm} = \left(\frac{-F_{p,top}}{\pi R_0^2 \dot{\epsilon}_0} - \frac{\rho g L_0}{2 \dot{\epsilon}_0} \right) e^{\dot{\epsilon}_0 t} - \frac{\sigma}{R_0 \dot{\epsilon}_0} e^{0.5 \dot{\epsilon}_0 t} - \frac{\rho \dot{\epsilon}_0 L_0^2}{2} \left(a + \frac{1}{4} \right) e^{2 \dot{\epsilon}_0 t} + \frac{\rho \dot{\epsilon}_0 R_0^2}{16} e^{-\dot{\epsilon}_0 t} \quad (8)$$

For the particular case of a stationary upper plate and a downwardly-accelerating lower plate we have $a = -1/2$. For this configuration, the additional term arising from correctly accounting for the acceleration of the reference frame thus changes not only the magnitude but also the sign of the dominant inertial correction term. Interestingly, we note that if a is set to be $-1/4$ (corresponding to upward motion of the top plate at $+\ddot{L}/4$ and downward motion of the lower plate at $-3\ddot{L}/4$) then the axial inertial term vanishes completely.

Another interesting analysis is to evaluate the effect of inertia on the spatial stress distribution in the filament. We consider again the flow in simple uniaxial elongation with constant strain-rate $\dot{\epsilon}_0$. The frame of reference is moving according to $z_0(t)$. Solution of the equations of motion then yields the following expressions for the stress distribution; for the stress difference $\tau_{zz} - \tau_{rr}$ we obtain

$$\langle \tau_{zz} - \tau_{rr} \rangle_z = \langle \tau_{zz} - \tau_{rr} \rangle_s + \rho(g + \ddot{z}_0)z + \frac{1}{2} \rho \dot{\epsilon}_0^2 z^2 \quad (9)$$

and for the radial pressure we find

$$p + \tau_{rr} = p_{external} + \frac{\sigma}{R_s} + \frac{1}{8} \rho \dot{\epsilon}_0^2 (R_s^2 - r^2) \quad (10)$$

In the above analysis we have assumed an initial rest state so that $\tau_{rr} - \tau_{\theta\theta} = 0$. From equations (9) and (10) we note that the principal stress difference $\tau_{zz} - \tau_{rr}$ changes quadratically with the axial co-ordinate. The radial variation is, however, decreasing during the experiment due to the fact that $R_s(t) \rightarrow 0$.

In real experiments where the no-slip boundary conditions at the rigid plates typically lead to a non-cylindrical shape, the so-called "wine-glass-stem", the inertia contribution becomes even larger than indicated by equation (9) due to the fact that more mass is located near the endplates. Computation of the inertial correction in equation (3) thus requires time-resolved measurements of the filament profile $R(z, t)$. In principle, it is also possible to exploit the exact cancellation of the axial inertial terms discussed above; however, this is impractical since it would require a stretching device having three locations with user-controlled displacement profiles (the two ends *and* the midplane) and the value of a would be time-varying because the profile of the filament changes in time.

A final limitation inherent in eq. (4) concerns the top-bottom symmetry implicitly assumed about the midplane of the elongating filament. For stretch rates less than $\dot{\epsilon}_{sag} \sim \rho g L_0 / (3\eta_0)$ gravitational sagging becomes increasingly important and there is a weak secondary axial flow within the filament in the direction of gravity. The volume of fluid remaining above the midplane at $x = 0$ (at which the local radius $R_s(t)$ is measured) is then $\int_0^{L/2} R^2 dx$ and this expression should replace the term $V_0/2$ in eq.(4). Like the

inertia integral, this term can also be computed from measurements of the filament profile $R(z, t)$. However it should be noted that the resulting tensile stress difference will contain contributions from both the imposed extensional flow and the induced gravitational ‘slumping’. It is difficult to deconvolute these two contributions without full numerical simulations.

References

- [1] S.L. Anna, McKinley, G.H., Nguyen, D.A., Sridhar, T., Muller, S.J., Huang, J. and James, D.F. An Inter-Laboratory Comparison of Measurements from Filament-Stretching Rheometers Using Common Test Fluids *J. Rheol.*, **45**(1):83–114, 2001.
- [2] G.H. McKinley and Sridhar, T.. Filament Stretching Rheometry of Complex Liquids. *Ann. Rev. Fluid Mech*, **34**:375–415, 2002.
- [3] P. Szabo. Transient filament stretching rheometer I: force balance analysis. *Rheol. Acta*, **36**:277–284, 1997.

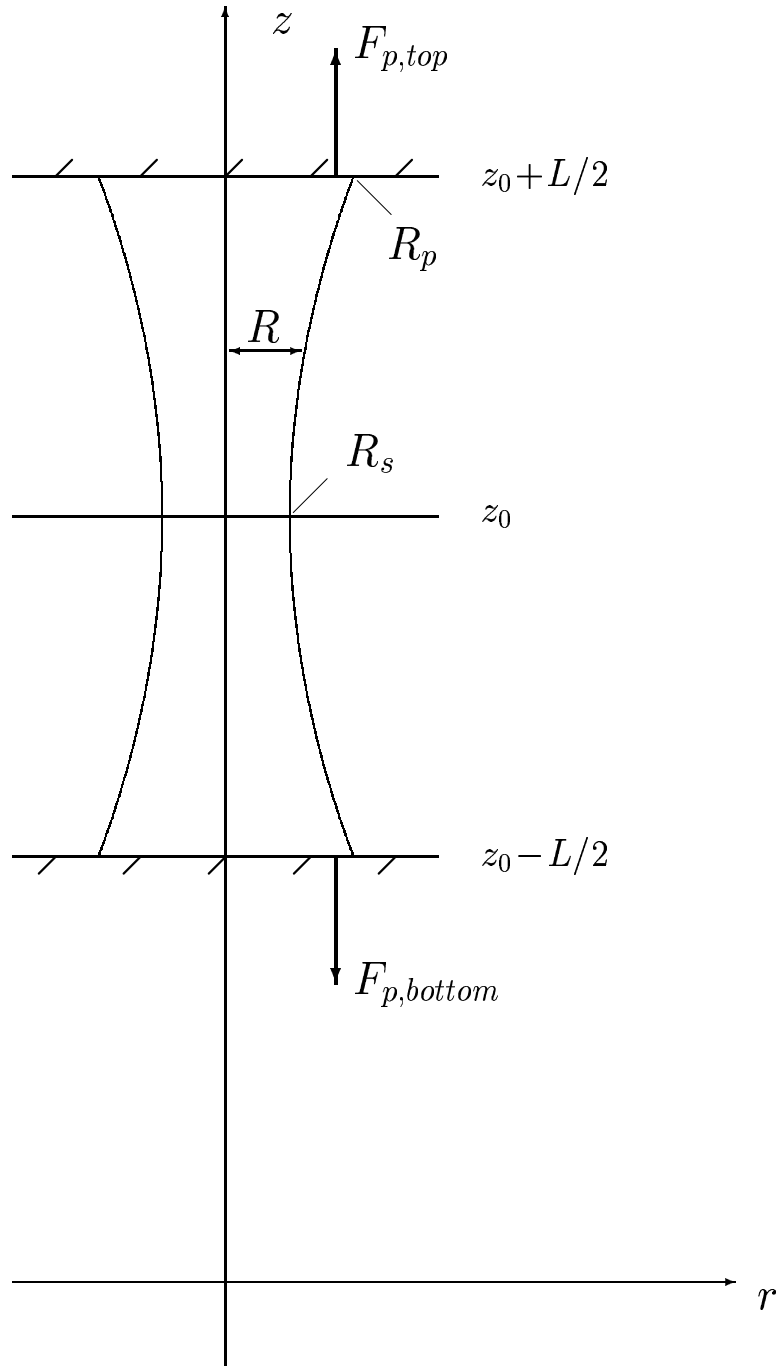


Figure 1: Definition of the basic variables in the filament geometry.